

NOISE AND NON-LINEARITY AS RELIABILITY INDICATORS OF ELECTRONIC DEVICES

J. Sikula, V. Sedlakova, P. Dobis

Brno University of Technology, Brno, Czech Republic

INVITED PAPER

MIDEM 2003 CONFERENCE

01. 10. 03 - 03. 10. 03, Grad Ptuj

Abstract: An application of noise and non-linearity measurements in analysis, diagnostics and prediction of reliability of electronic devices is discussed. The sensitivity of noise and non-linearity to the device defects and other irregularities is typical feature of these methods. Conceptions of $1/f$ noise, burst or RTS noise, thermal noise and third harmonic voltage are described and their explanation is done. The results of noise and non-linearity measuring are shown. Possible reliability indicators for conducting film resistors, MOSFETs and quantum dots are presented.

Šum in nelinearni efekti kot pokazatelji zanesljivosti elektronskih komponent

Izvleček: V prispevku pokažemo uporabo meritev šuma in nelinearnosti pri analizi, diagnozi in napovedi zanesljivosti elektronskih komponent. Glavna odlika tega pristopa je ravno občutljivost šuma in nelinearnosti na napake in druge nepravilnosti znotraj komponente. Opišemo in razložimo koncept $1/f$ šuma, RTS šuma, termičnega šuma in tretje harmonske napetosti, kakor tudi obrazložimo rezultate meritev. Predstavimo možne pokazatelje zanesljivosti prevodnih plasti, uporov, MOSFET tranzistorjev in kvantnih lukenj.

1. Introduction

The noise spectroscopy in time and frequency domain is one of the promising methods to provide a non-destructive characterisation of semiconductor materials and devices. This applies to both active and passive components, i.e., bipolar, quantum dots and MOS structures, on one hand, and resistors and capacitors on the other. As a main diagnostic tool it is proposed to use low frequency current or voltage noise spectral density and their statistical distributions.

The noise in a device, correlation with reliability and why conduction noise, especially $1/f$ noise, is a quality indicator for devices is indicated in [1]. Here we restrict ourselves to $1/f$ noise as a diagnostic tool in resistance type devices. The knowledge about $1/f$ noise is based on experimental facts that fit into the empirical relation for the $1/f$ noise with the Hooge-parameter α .

There are two kinds of $1/f$ noise in electronic devices. The first type was called the fundamental $1/f$ noise. It may be associated with the $1/f$ noise that is caused by the carrier mobility fluctuations at the charge-carrier scattering by phonons [1]. The other kind of $1/f$ noise is generated by defects in the device. It was called as excess $1/f^\alpha$ noise and it is a characteristic for detecting of imperfections and latent defect. This kind of excess $1/f^\alpha$ noise may be the non-equilibrium $1/f$ noise [2, 3].

It is known that most of failures result from the latent defects created during the manufacture processes or during the operating life of the devices. The sensitivity of excess electrical noise to this kind of defects is the main reason of investigation and use of noise as a diagnostic and prediction tool in reliability physics for the semiconductor devices lifetime assessment. The noise spectral density depends on stress and damage and varies among nominally identical devices.

The sensitivity of the noise characteristics to the structure defects and other irregularities is typical feature of these methods. It is due to microphysical origin of fluctuation caused by quantum transitions of charge carriers. Noise depends on: i) perfection of the crystal structure, number of grain boundaries, point defects, linear defects, ii) surface parameters and iii) homogeneity and manufacturing quality of the device active region.

The actual reliability of electronic devices is usually less than the maximum theoretical value of reliability depending on the attained manufacture level. It may be due to irregularities in the manufacturing processes. It was observed that chemical condition of the surface could affect the magnitude of the noise spectral density.

In the present paper the application of noise spectroscopy on thin and thick conducting film resistors, MOSFETs and quantum dots and is given. The noise characteristics variation during stress and ageing are much larger than

those of the DC characteristics and then our experimental studies are used for a quality and reliability assessment.

2. Characterisation of the noise

Noise generated in semiconductor sample consists from thermal noise, burst or RTS noise, generation-recombination (GR) noise, $1/f$ noise and $1/f^2$ noise. There are two experimental ways to characterize fluctuations in semiconductor sample. The first is based on the analyses of stochastic process realization in time domain. In this case average value, probability density and distribution function can be obtained. The second one uses Fourier transformation of time domain realization and gives information about second order statistical moments as is noise spectral density. The stochastic process realization is then analysed in frequency domain. This method is frequently used and noise sources are characterized by frequency dependence of noise spectral density. Noise voltage, current, and power spectral densities are used. We give short description of them.

2.1 Thermal noise

All semiconductor samples always display thermal noise caused by random motion of the charge carriers and their interaction with phonons. The spontaneous fluctuations across the resistor have a white noise spectrum given by:

the voltage noise spectral density

$$S_u = 4kTR \quad (1)$$

the current noise spectral density

$$S_I = 4kTG \quad (2)$$

or the power noise spectral density

$$S_p = S_u / R = S_I R = 4kT \quad (3)$$

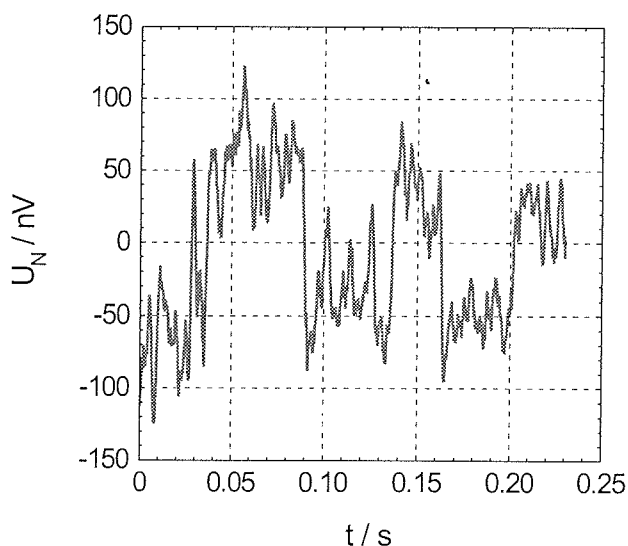


Fig.1. RTS noise voltage time dependence

where k , T and R are Boltzmann constant, the absolute temperature, and the sample resistance respectively. The thermal noise of resistors is often used to calibrate the noise-measuring set-up. The thermal noise from a biased sample is proportional to a temperature, which is larger than a substrate temperature due to Joule heating. The thermal resistance is an important indicator of delamination of the thick film layer and hence an indicator of early failures. Thus a strong increase in thermal noise under bias goes hand in hand with an increased risk of failures.

2.2 Burst or RTS noise

This type of noise is called burst or random telegraph signal (RTS) noise. It is an important indicator of a single trap activity in a small subsystem with a small number of free carriers. Such defect often appears due to laser trimming. Defect region has small dimensions and is submitted to high electric field current density. Therefore it often degrades faster and at least shows a poor noise behaviour. Time realisation of voltage fluctuation on resistor is given in Fig. 1. and noise spectral density of this type of noise for the resistor $R = 8 \text{ k}\Omega$ is shown in Fig.2 for applied voltage 0.7 and 1.4 V.

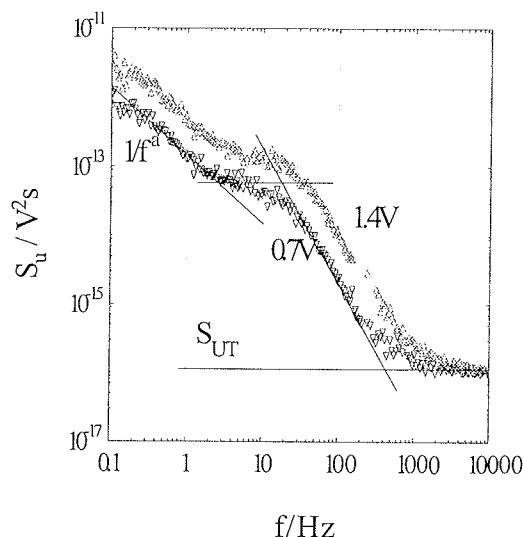


Fig.2. Noise spectral density vs. frequency

2.3 Generation-recombination noise

Generation-recombination (G-R) noise is a fluctuation in the conduction, and like burst noise is caused by the carriers number fluctuations. The amplitude density distribution is Gaussian with the Lorentzian spectrum for simple transitions between a band and traps at one energy level. Traps energy level must be near to Fermi level in order to create G-R noise. That is the reason why some devices can show G-R noise just in a certain temperature range.

2.4 Noise of $1/f$ type

Present theories of $1/f$ noise assume that there are two sources: fundamental $1/f$ noise and excess $1/f^2$ noise. According to Hooge [1], $1/f$ noise is due to carrier mobility

fluctuations and current noise spectral density is given by a generalised Hooge's formula

$$S_I = \alpha \cdot I^2 / f \cdot N \quad (4)$$

where S_I is the current noise spectral density, f is frequency, N is the total number of carriers in the sample active region, I is the device current and α is an empirical constant. Hooge constant α is now extensively used to characterise the device structure perfectness. The values of α measured on the devices ranges from 10^{-3} (poorest samples) to 10^{-7} (currently the best samples).

Normalised noise spectral density with respect to applied voltage S_U/U^2 , electric current S_I/I^2 or resistance S_R/R^2 can be expressed by

$$S_U/U^2 = S_I/I^2 = S_R/R^2 = \alpha / f \cdot N \quad (5)$$

Normalised noise spectral density for samples with different widths and lengths 0.3mm, 0.5mm and 1mm is shown in Fig.3.

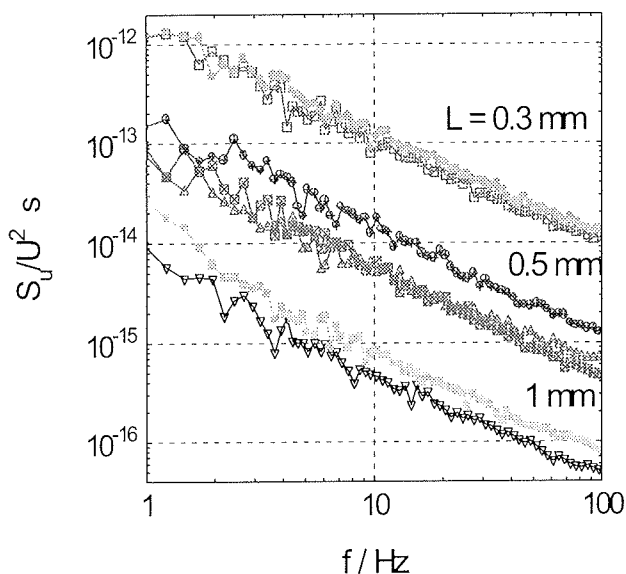


Fig. 3. Normalised voltage noise spectral density for thick film resistors

It was proposed to defined the quality and reliability indicator C_Q as

$$C_Q = S_I / I^2 \quad (6)$$

Normalised frequency curve of C_Q indicator is shown in Fig.4. The better technology, the lower C_Q value and its dispersion is measured.

At present the concept of the excess noise as a quality and reliability indicator is generally used. There is also a variety of measuring set-ups and measuring conditions. Not all of them provide the best attainable resolution. Generally speaking, one has to be able to distinguish the excess noise of the device, which carries information on the device condition, from the background noise.

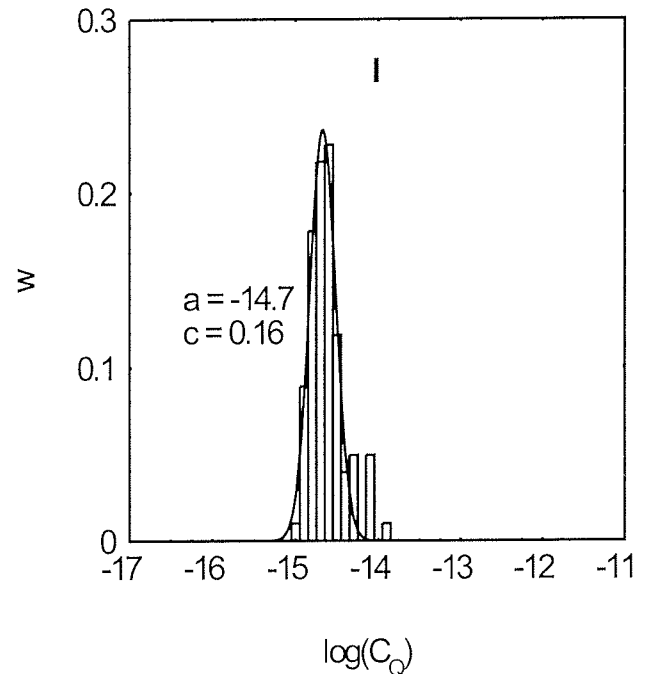


Fig.4. Normalised frequency curve of C_Q indicator

2.5 Power noise spectral density

This quantity corresponds to voltage or current fluctuation on sample resistance R . From this point of view behaviour of resistor type devices can be described by similar model as was given by Hooge for monocrystals [1].

We propose, that power noise spectral density S_P is proportional to power dissipated by one charge carrier P_0 and inversely proportional to frequency

$$S_P = \alpha P_0 / f \quad (7)$$

where

$$P_0 = e \mu E^2 \quad (8)$$

α is proportionality constant, μ is charge carrier mobility, E is electric field intensity.

Total power noise spectral density including thermal noise will be given by

$$S_P = 4kT + a_\mu e E^2 / f \quad (9)$$

where a_μ has a unit of mobility and is given by

$$a_\mu = \alpha \cdot \mu \quad (10)$$

Quantity a_μ does not depend on sample length and width as is shown in Fig. 6.

Power noise spectral density has lowest value $S_P = 4kT$ as is shown in Fig. 5.

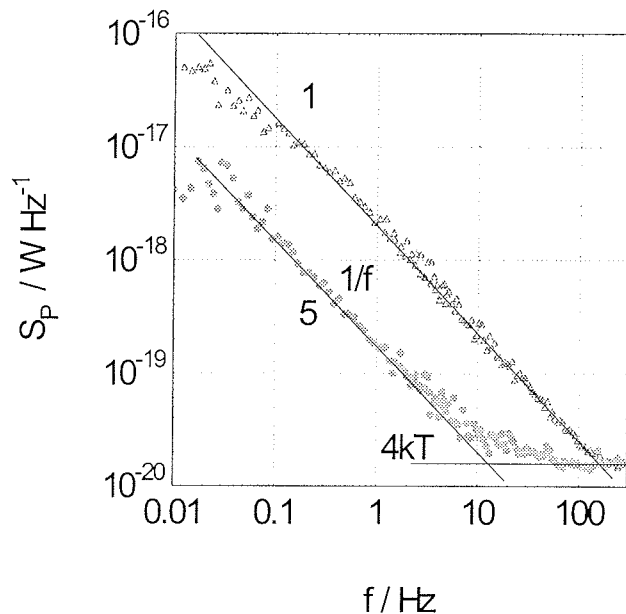


Fig. 5. Power noise spectral density for two thick film resistors

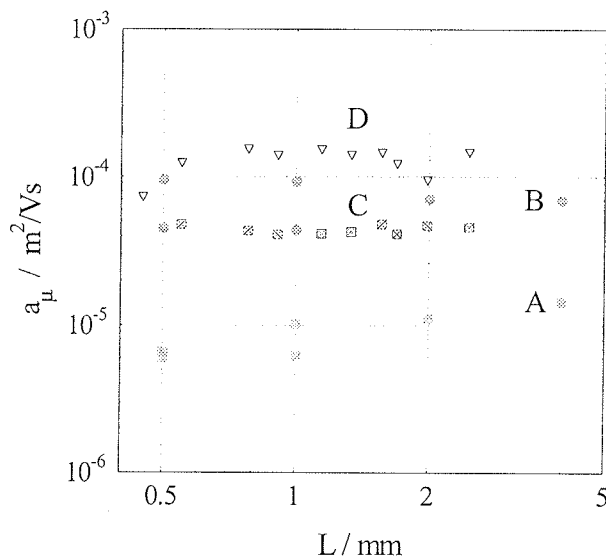


Fig. 6. Quantity a_m for pastas 10 kΩ/ and different technologies

2.6 The non-equilibrium resistance fluctuations

The resistance of any conducting two-terminal devices $R(I, t)$ is generally a non-linear function of a current I and can be approximated by:

$$R(I, t) = R_0(t) + \sum_{n=1}^{\infty} R_n(t) I^n(t) \quad (11)$$

Here, the time dependence of coefficients $R_n(t)$ ($n = 0, 1, 2, \dots$) represents the fluctuations in the resistance. For a weakly non-linear sample the terms in (11) decrease rapidly with n so that for ordinary working currents the voltage fluctuations $\Delta U(t)$ across a sample under a DC current I_0 , with accounting of the first three terms in (11), given by

$$\Delta U(t) = \Delta R(I, t) I_0 = \Delta R_0(t) I_0 + \Delta R_1(t) I_0^2 + \Delta R_2(t) I_0^3 \quad (12)$$

where $\Delta U(t) = U(t) - \bar{U}$ and \bar{U} is the time-averaged voltage drop across the sample. Here fluctuations of the terms in (11) are

$$\Delta R_n(t) = R_n(t) - \bar{R}_n \quad (n = 0, 1, 2), \quad (13)$$

where \bar{R}_n are the time-averaged coefficients. Fluctuations $\Delta R_0(t)$ give the equilibrium $1/f^a$ noise. Fluctuations $\Delta R_1(t)$ and $\Delta R_2(t)$ are sources of the non-equilibrium resistance fluctuations. When the noise spectral density $S_U(f)$ is measured under DC current, the equilibrium and non-equilibrium components are superimposed. If the DC current is small the non-equilibrium component is hidden by the equilibrium one.

2.7. Measuring set-up

There is a variety of measuring set-ups and measuring conditions. Not all of them provide the best attainable resolution. Generally speaking, one has to be able to distinguish the excess noise of the device, which carries information on the device condition, from the background noise. To get a good measurement resolution, it is necessary to carry out the measurements in the region, where the expected noise component magnitude is distinctly higher than that of the background.

3. Non-linearity

The resistor structure consists of metallic grains and inter-grain layers with semiconductor conductivity. Junctions between metal grain and semiconductor layer are non-ohmic. Important non-ohmic regions are at contacts and in vicinity of defects of resistor structure.

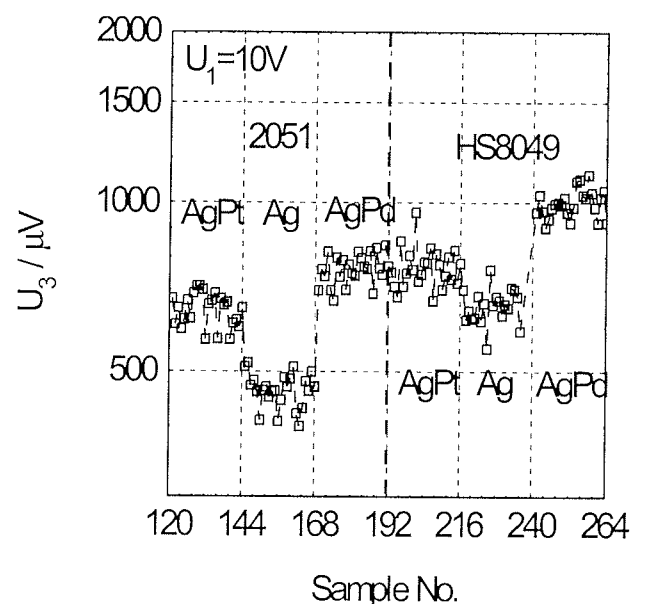


Fig. 7. Third harmonic voltage for samples 0.3x0.3mm, paste 100kΩ/□ at $U_1=10V$

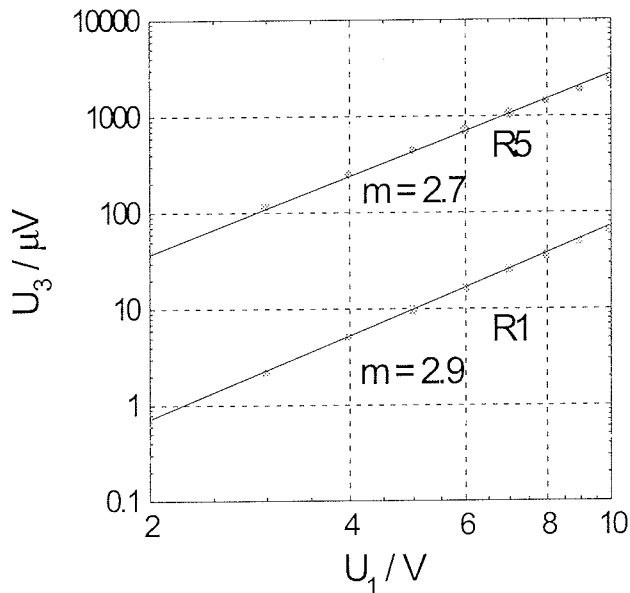


Fig. 8. Third harmonic voltage as a function of first harmonic voltage

These non-ohmic regions are screened by the third harmonic voltage measurement. This non-destructive method gives additional information on the reliability of passive devices. The basic measuring frequency was 10 and 100 kHz and nonlinearity index was defined as ratio of the third harmonic and the first harmonic applied voltage, expressed in dB:

$$NLI = 20 \log(U_3/U_1) \quad (14)$$

Third harmonic voltage (THV) as a function of first one U_1 was experimentally studied for different resistors and all cases the U_3 is proportional to the U_1^3 as is shown in Fig. 8.

Non-linearity measurements for different resistor technologies show, that the third harmonic voltage U_3 is dependent on the type of resistor and the contact electrode material (Figs. 7.). The third harmonic voltage U_3 dependence electric field intensity E_1 or current density is shown in Figs. 9. and 10. U_3 is proportional to the third power of the electric field intensity or current density. Proportionality constant depends on the given thick film resistor technology (see curve A for AgPd and B for Ag conductors).

Absolute value of THV can be taken as reliability indicator only for devices produced by the same technology. If the resistor exhibits either a contact non-linearity or a current crowding problem then the THV will depend on current density peak. It was observed, that thick film resistors with AgPd contact electrode have higher value of third harmonic voltage, but show better long term stability and reliability comparing with Ag contact electrode resistors. In this case non-homogeneities in current density distribution are responsible for higher values of non-linearity and noise spectral density. Silver diffusion from contact electrode into the resistive layer results to the increase of conductivity of resistive layer, and then the peak of current density is shifted

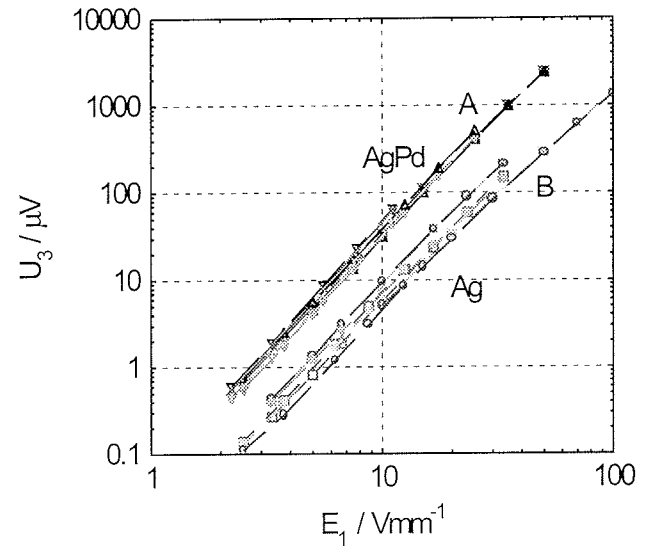


Fig. 9. THV as a function of electric field intensity for Ag and AgPd contacts

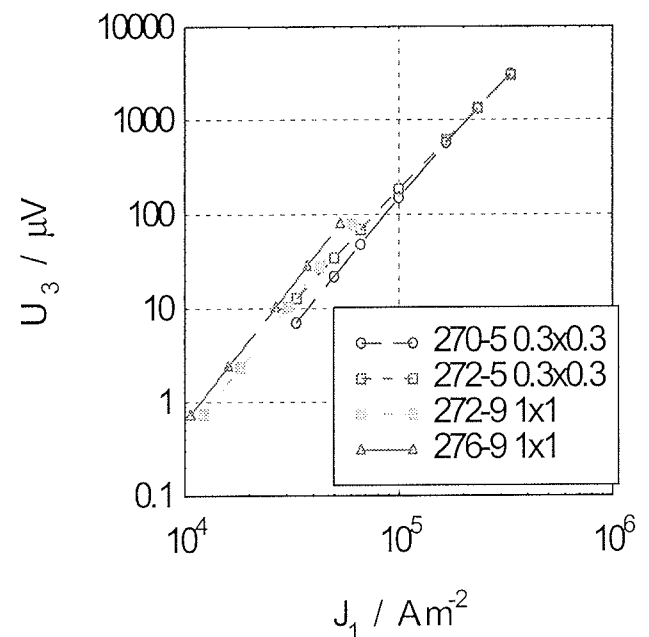


Fig. 10. THV as a function of current density for Ag/Pd contacts

from contact - resistor interface into resistor volume. In this case the noise and non-linearity dominant sources are not on the contact - resistor interface, but are shifted to the thick film resistor volume. The contact - thick film interface is not so much affected by Joule heating of this spot and we suppose that irreversible processes on contact interface are weaker.

4. Thin and thick film resistors

Low frequency noise and non-linearity measurements are used as reliability indicators to describe ageing stability of film resistors. In order to detect technology step responsi-

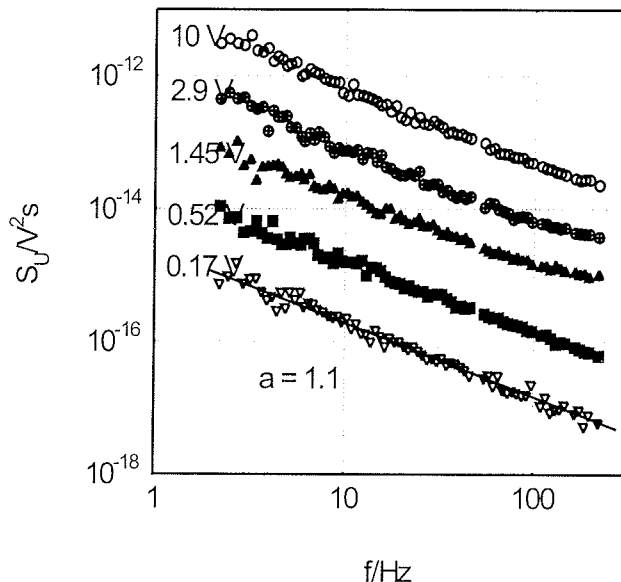


Fig. 11. Noise voltage spectral density vs. DC applied voltage for metallic resistor

ble for noise sources creation, in co-operation with some manufacturers, studies were performed at three different stages of the technology process: resistance layer deposition, laser adjustment and protective layer coating. Critical is laser adjusting operation, when cracks and defects can be generated, which are sources of noise.

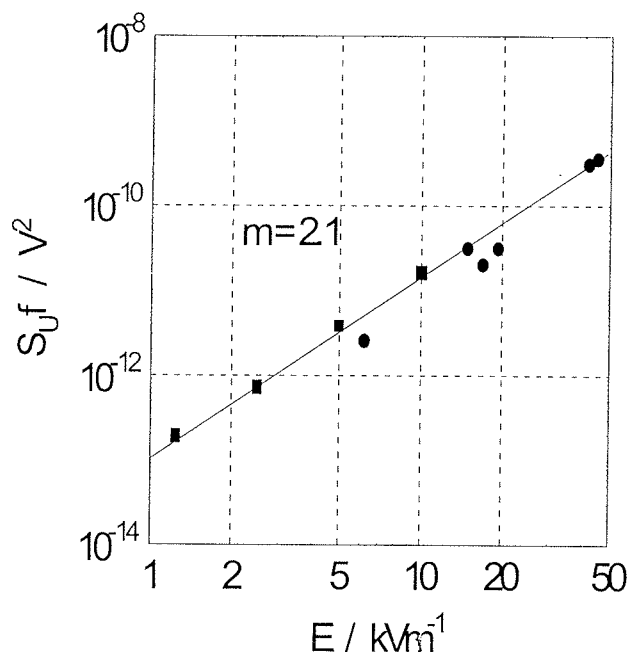


Fig. 12. $1/f$ noise spectral density versus electric field intensity

Noise spectral density as a function of frequency for different values of DC applied voltage of metallic resistor is shown in Fig. 11. All curves have the slopes varying from $a=1.0$ to 1.1 . Normalized $1/f$ noise spectral density versus electric field intensity for thick film resistor is shown in Fig. 12.

Quadratic dependence of noise spectral density on electric field intensity or applied voltage is characteristic for stationary ergodic stochastic processes.

4.1 Non-homogeneous current density distribution

The contact electrode material of the thick film resistors has important influence on their quality and reliability. Strong dependence of non-linearity and noise on the contact electrode material was observed [5]. Thick film resistors with AgPd contact electrode have higher value of third harmonic voltage, but show better long term stability and reliability comparing with Ag contact electrode resistors. We determined from the SEM analyses, that the sharpness of AgPd contact electrode is higher than Ag contact electrode one. Modelling of the current distribution for different sharpness of metallic contact cross sections was performed and it shows that the electrode geometry plays dominant role for current distribution in thick film resistor layer.

If the thick film resistor exhibits either a contact noise or a current crowding problem on a microscopic scale or both, then the calculated α from (4) will not be the α -value representing the $1/f$ noise properties of the thick film material. These will lead to higher α values. Sources of this excess noise are current crowding near the contacts. The $1/f$ noise parameter α_a value is higher than 3×10^{-3} .

Due to the silver diffusion conductivity between Ag contact and resistive layer varies continuously. The conductivity of resistor layer in the vicinity of contact decreases from the silver conductivity to reach the conductivity of resistive paste. For the comparison also the model without the transition region was analysed. The peak of the electric field intensity is shifted into resistor volume with respect to model without Ag diffusion (see Fig. 13.)

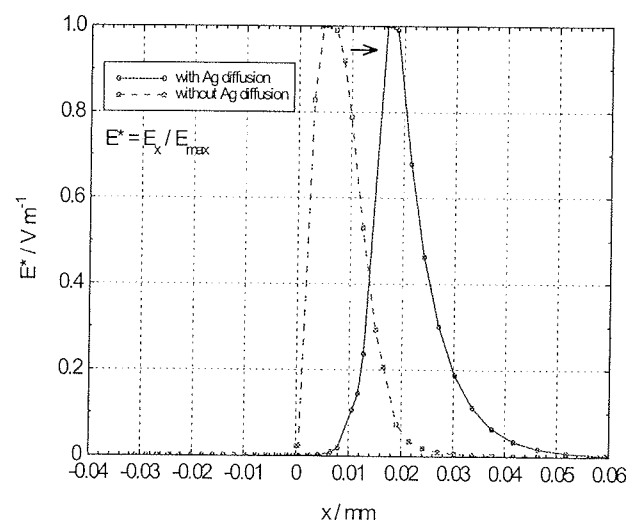


Fig. 13. Shift of electric field intensity near contact due to silver diffusion

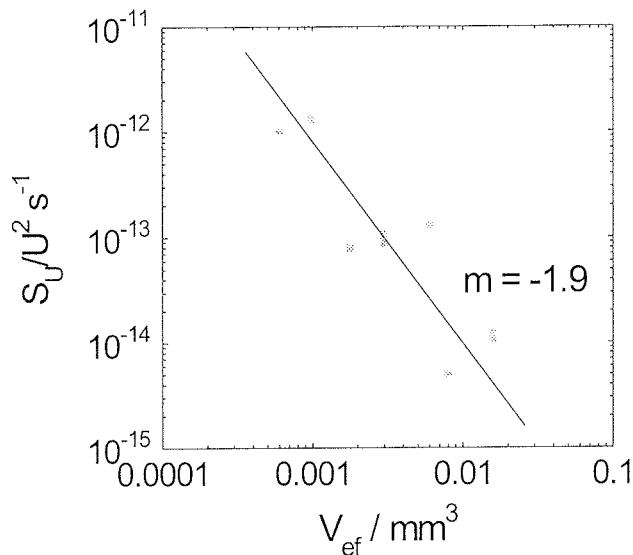


Fig.14. Normalised noise spectral density versus resistor effective volume

The silver diffusion in resistor volume causes shift of current density peak from the contact – resistor interface. This effect leads to lower stability of resistor characteristics due to ageing, but noise and non-linearity characteristics are reduced. The current density peak in the vicinity of contact affects the values of noise and non-linearity characteristics, but they are not connected with irreversible processes at the contact interface. In this case the higher value of noise or non-linearity does not indicate lower reliability.

4.2 Noise and sample volume

Normalised noise spectral density increases with decreasing sample volume. Small sample has higher value of noise spectral density. We found that noise spectral density is inversely proportional to the square of thick film sample volume (see Fig.14.). This result is not in coincidence with linear dependence predicted by Hooge empirical model $/4/$. We suppose that this effect is a result of non-homogeneous electric field and current crowding enhances. Decreasing the sample length the current density peak near contacts is more pronounced.

5. RTS in mosfets and quantum dots

It is supposed to be caused by individual traps, which can be either in silicon, or the oxide, or in the interface between the silicon and the oxide. Its position results on the time of the RTS pulses. For the trap located in the channel or in the boundary between the oxide and silicon at the gate side, the mean pulse time for an n-type semiconductor with a carrier concentration of 10^{16} cm^{-3} , the capture cross section 10^{16} cm^2 and a thermal velocity of 10^7 cm/s is 0.1 microseconds.

If the trap is located in the oxide then the capture τ_c and emission τ_e time constants will be longer because of tun-

nelling. The tunnelling time increases with the trap depth exponentially and for a depth of 1 nm the characteristic time is of the order of 1 second. The capture time τ_c is inversely proportional to the square of the drain current I_D as is shown in Fig. 15. The emphasis is on those signals showing a capture process, which deviates from the standard Shockley-Read-Hall kinetics corresponding to a quadratic dependence on the number of carriers or on the current.

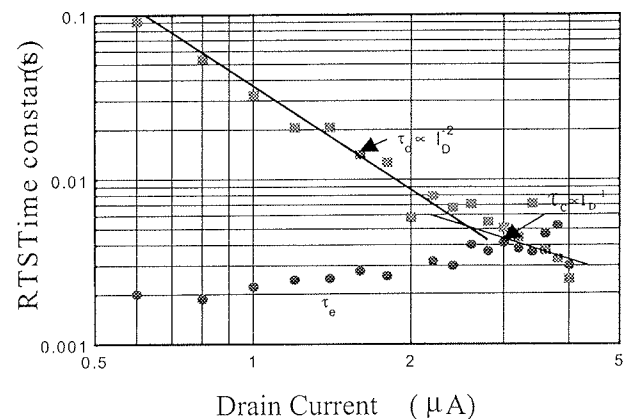


Fig. 15. Capture τ_c and emission τ_e time constants

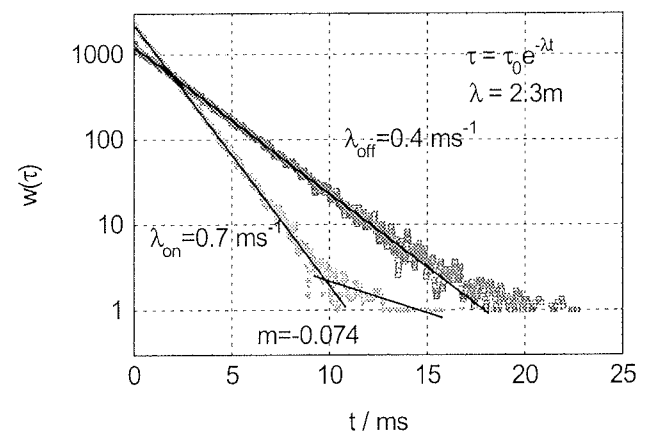


Fig. 16. Capture τ_c and emission τ_e time probability density for sample N31

Time constant distribution is exponential in first approximation only and result for a small-area Si n-MOSFET is in Fig. 16. This is second experiment on which a modified two-step approach is proposed. It includes the capture of a carrier by a trap located at the Si-SiO₂ interface, followed by a tunnelling process of the trapped carrier between the interface trap and a trap located in the SiO₂ layer. Generation-recombination process has noise spectral density Lorentzian type as is shown in Fig. 17. By this model a quadratic dependence of the capture rate on the drain current can be explained, provided that the quasi-Fermi level at the surface is below the interface trap level. Noise spectral density reach maximum value (see Fig. 18) for current at which Fermi quasi level coincide with trap energy level. From these experiments the interface trap cross-

section and oxide trap cross-section can be determined. This result is based on assumption that noise is caused by charge carrier quantum transitions.

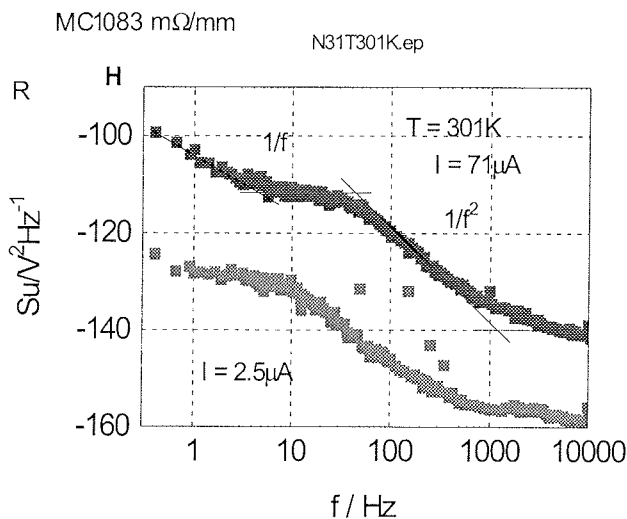


Fig. 17. Noise spectral density of n-MOSFET

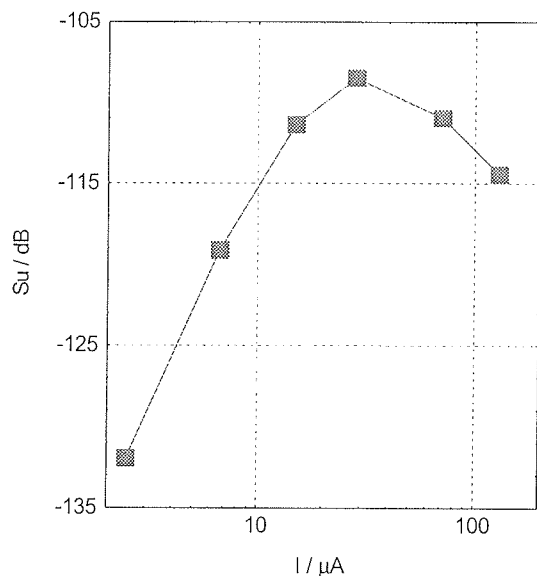


Fig. 18. Su vs. drain current

5.1 Quantum Dots

Quantum dot (QD) structures have attracted much attention because of interest in not only the relevance of low-dimensional electron gas physics but also future applications of high-density, low power, and highly functional integrated circuits. Tacano et al. /6/ fabricated an AlGaAs/InGaAs heterojunction field-effect transistor (FET) memory cell in a tetrahedral-shaped recess (TSR) structure, which has a hole-trapping QD as a floating gate, and succeeded in observing RTS noise in the retention characteristics of the memory cell. RTS observed in short- and narrow-channel FET are direct evidence of a single charge capture and emission. An analysis of RTS in this work quantitatively explains details of hole trapping processes in the TSR QD.

Temperature dependent RTS pulses (Fig.19.) are excited up to 130 K, and the activation energy of a hole capture and emission processes were estimated as:

$$Et_1 = 190 \text{ meV and } Et_2 = 260 \text{ meV.}$$

Similar value of the activation energy was found in MOS structures (see Schulz /7/)

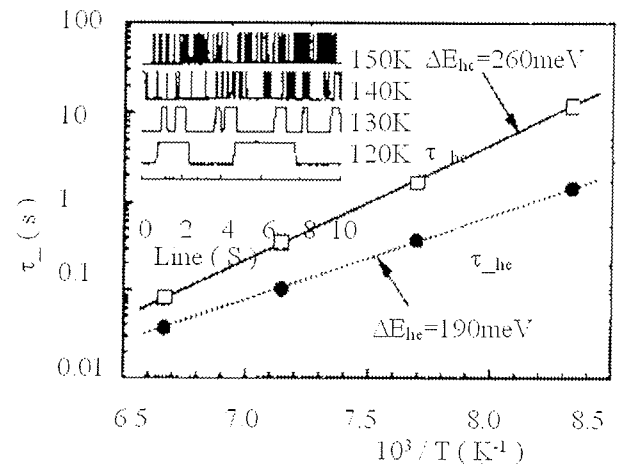


Fig. 19. RTS from QDs at various temperatures

6. Conclusion

It was proposed as a quality and reliability indicator a normalised $1/f$ noise spectral density and non-linearity index. Burst noise component shows that the thick and thin conducting layers are composed of chainlike structure of metal grains separated by semi-conducting or insulating layers.

Power noise spectral density of $1/f$ noise is proportional to power dissipated by one charge carrier and inversely proportional to frequency. We may conclude that there are two effective carrier mobilities: one for the transport and the other for the noise characterization. RTS noise amplitude has its maximum value when the electron Im_{ref} coincides with the trap energy level. Then in quantum dots and MOS structures the RTS noise appear in a short temperature range. All models presented up to now can explain the bistability of the system, which is caused by defects in the device structure.

Acknowledgement

This research was supported by the KONTAKT Czech - Japan Government Cooperation Grant Me-605 and by the Grant MSMT: Microsynt No 2622 00022.

References

- /1./ F. N. Hooge, T. G. M. Kleinpenning, and L. K. J. Vandamme, "Experimental studies on $1/f$ noise," *Reports on Progress in Physics*, vol. 44, no. 5, pp. 479-532, May1981.

- /2./ G. P. Zhigal'skii, A. V. Karev, *J. Communications Technology and Electronics* **44** (1999) 206-210
- /3./ L. K. J. Vandamme, "On the Calculation of 1/f Noise of Contacts," *Applied Physics*, vol. 11 pp. 89-96, 1976
- /4./ L. K. J. Vandamme, "Noise as a Diagnostic Tool for Quality and Reliability of Electronic Devices," *IEEE Transactions on Electron Devices*, vol. 41, no. 11, pp. 2176-2187, Nov.1994.
- /5./ V. Sedlakova et al., Current Density Distribution, Noise and Non-linearity of Thick Film Resistors, *CARTS US Scotsdalle March 31, 2003*.
- /6./ 14. Y. Awano, M. Shima, Y. Sakuma, Y. Sugiyama, N. Yokoyama and M. Tacano, Temperature controlled RTS noise from a single InGaAs quantum dot, Proc. of the Int. Conf. "Noise in Physical Systems and 1/f Fluctuations", Gainesville, FL, USA (2001) p.359
- /7./ M. Schulz and A. Pappas, Telegraph noise of individual defects in the MOS interface, Proc. of the Int. Conf. "Noise in Physical Systems and 1/f Fluctuations", Kyoto, p. 265 (1991)

J. Sikula, V. Sedlakova, P. Dobis
Brno University of Technology, Technická 8,
602 00 Brno, Czech Republic
Tel/Fax +4205 4114 3398,
E-mail: sikula@feec.vutbr.cz

Prispelo (Arrived): 15.09.2003 Sprejeto (Accepted): 03.10.2003